

# Os(VIII) doping effects on the properties and crystalline perfection of potassium hydrogen phthalate (KHP) crystals

K. Muthu · G. Bhagavannarayana ·  
C. Chandrasekaran · S. Parthiban ·  
S. P. Meenakshisundaram · S. C. Mojumdar

CTAS2009 Special Chapter  
© Akadémiai Kiadó, Budapest, Hungary 2010

**Abstract** The effect of dopant, Os(VIII) on the growth process, crystalline perfection and properties of potassium hydrogen phthalate (KHP) single crystals grown by a slow evaporation solution growth technique has been investigated. The XRD analysis of black-colored doped specimen reveals slight structural changes as a result of doping. The SEM images exhibit defect centers and crystal voids. The complex formation of KHP with Os(VIII) is evidenced by the considerable shift in  $\lambda_{\max}$  of the doped specimen and enhanced fluorescence intensity is observed by doping. Differential scanning calorimetry (DSC) and TG-DTA studies reveal the purity of the sample and no decomposition is observed up to the melting point. The high resolution X-ray diffraction (HRXRD) studies used to evaluate the crystalline perfection reveal some features on the capability of accommodating the dopant in the crystalline matrix. The diffraction curve (DC) patterns indicate that the high valence transition metal predominantly occupies the interstitial positions and the doping depresses the second harmonic generation (SHG) efficiency owing to the deterioration of crystalline perfection disturbing the charge transfer and nonlinearity.

---

K. Muthu · C. Chandrasekaran · S. Parthiban ·  
S. P. Meenakshisundaram  
Department of Chemistry, Annamalai University,  
Annamalainagar 608 002, India

G. Bhagavannarayana  
Materials Characterization Division, National Physical Laboratory, New Delhi 110 012, India

S. C. Mojumdar (✉)  
Department of Engineering, University of New Brunswick,  
Saint John, NB E2L 4L5, Canada  
e-mail: scmojumdar@yahoo.com;  
subhash.mojumdar@utoronto.ca

**Keywords** HRXRD · Nonlinear optical properties · Osmium · Potassium hydrogen phthalate

## Introduction

Potassium hydrogen phthalate (KHP) crystal is well known for its application in the production of crystal analyzer for long wave X-ray spectrometer [1, 2]. KHP possesses piezoelectric, pyroelectric, elastic, and nonlinear optical properties [3–5]. It crystallizes in orthorhombic structure with space group  $Pca2_1$  [6]. It has platelet morphology with perfect cleavages along (010) plane. Using the periodic bond chain analysis, the morphology of KHP has been determined [7]. Recently, KHP crystals are used as substrates for the growth of highly oriented film of conjugated polymers with nonlinear optical susceptibility [8, 9]. KHP is chosen as model compound because of its well-developed surface pattern on the (010) face consisting of high and very low growth steps which can be relatively easily observed by means of optical microscopy [10, 11].

The elements most used as surface modifier in the development of electro catalytic materials have been chosen from the platinum group, mainly osmium. Osmium is a lustrous and silvery metal. The metal is used in a few alloys and in industry as a catalyst. It shows a good hardness, a capacity to assume a great number of oxidation states (+II to +VIII). The easier adsorption of oxygenated species on this metal than platinum is the main reason for its numerous applications [12].

Recently, we have investigated the influence of alkaline earth and transition metals doping on the properties and crystalline perfection of KHP crystals [13]. It is interesting to observe that the alkaline earth metal Mg occupies

predominantly substitutional positions while the transition metal Hg mainly occupies the interstitial sites. Accommodating capability of ADP crystals with dopants like KCl and oxalic acid reveals some interesting features [14]. Influence of Mn(II) doping on the NLO properties of ZTS reveals a good correlation of SHG efficiency and the crystalline perfection [15]. Thermal, microscopic, X-ray, and spectral analyses are very important methods in materials characterization. Therefore, many authors have applied these techniques for various materials characterization [16–42]. This study has been undertaken as a continuation of our studies to ascertain the influence of doping the metals on the properties and crystalline perfection. As per our knowledge this is also the first detailed report of osmium doping dealing with crystalline perfection and non-linear optical (NLO) properties in technologically important crystals.

## Experimental

### Synthesis and crystal growth

KHP crystals were grown by a slow evaporation solution growth technique in this study. Recrystallized salt of KHP (E. Merck) was taken as raw material. A saturated aqueous solution of KHP was prepared (12 g per 100 mL). Osmium tetroxide (Aldrich), OsO<sub>4</sub>, is highly toxic. Concentrations in air as low as 10<sup>-7</sup> g m<sup>-3</sup> can cause lung congestion, skin damage, and severe eye damage. Calculated quantity of OsO<sub>4</sub> is dissolved in 0.05 N NaOH solution and this solution is used for doping studies. The seed crystals are allowed to float on the surface of the aqueous saturated solution and left for slow evaporation at room temperature (30 °C). The prepared solution was filtered with a micro-filter. The crystallization took place within 15–20 days and the crystals were harvested when they attained an optimal size and shape. The growth rate of crystals is high with low concentration of dopants while decreased with an increase in dopant concentration. Quite likely, at high concentrations of the dopant, the adsorption film blocks the growth surface and inhibits the growth process [43, 44]. Bulk crystals are grown using optimized growth parameters. High quality transparent crystals were harvested from the growth medium in the presence of low concentrations of dopants. Photographs of the as grown doped and undoped crystals are shown in Fig. 1.

### FT-IR spectra

The FT-IR spectra were recorded for all the samples including pure KHP using an AVATAR 330 FT-IR instrument using the KBr pellet technique in the range 500–4,000 cm<sup>-1</sup>.



**Fig. 1** Photographs of KHP as-grown crystals **a** pure and **b** 1 mol% OsO<sub>4</sub> doped

### Powder XRD

Powder XRD analysis was performed using a Philips Xpert Pro Triple-axis X-ray diffractometer. The XRD data is analyzed by Rietveld method with RIETAN-2000.

### SEM

The surface morphology was observed using a JEOL JSM 5610 LV scanning electron microscope. In the SEM, the image is formed and presented by a very fine electron beam, which is focused on the surface of the specimen. At any given moment, the specimen is bombarded with electrons over a very small area.

### Fluorescence (PL) spectra

Fluorescence spectral study was carried out using a spectrofluorophotometer, RF-5301 PC SHIMADZU.

### Thermal analysis

Simultaneous TG–DTA–DSC curves were recorded on a SDT Q600 (TA instrument) thermal analyzer. The TG–DTA curves were simultaneously obtained in nitrogen at a heating rate of 10 °C min<sup>-1</sup>. The DSC analysis of crystals

grown from pure and Os(VIII)-doped KHP solutions was carried out between 50 and 400 °C in the nitrogen atmosphere.

#### Kurtz powder SHG measurements

The SHG test on the crystals was performed by the Kurtz powder SHG method [45]. An Nd:YAG laser with modulated radiation of 1,064 nm was used as the optical source and directed on the powdered sample through a filter. The grown crystals were ground to a uniform particle size of 125–150 µm and then packed in a micro capillary of uniform bore and exposed to laser radiation. The output from the sample was monochromated to collect the intensity of the 532 nm component and to eliminate the fundamental. Second harmonic radiation generated by the randomly oriented micro crystals was focused by a lens and detected by a photo multiplier tube.

#### High-resolution X-ray diffractometry

To reveal the crystalline perfection of the grown crystals and to study the effect of dopants added in the saturated aqueous solution during the growth process, a multicrystal X-ray diffractometer developed at NPL [46] has been used to record high-resolution rocking or diffraction curves (DCs). In this system a fine focus ( $0.4 \times 8$  mm; 2 kW Mo) X-ray source energized by a well-stabilized Philips X-ray generator (PW 1743) was employed. The well-collimated and monochromated MoK $\alpha_1$  beam obtained from the three monochromator Si crystals set in dispersive (+, -, -) configuration has been used as the exploring X-ray beam. This arrangement improves the spectral purity ( $\Delta\lambda/\lambda < 10^{-6}$ ) of the MoK $\alpha_1$  beam. The divergence of the exploring beam in the horizontal plane (plane of diffraction) was estimated to be  $\ll 3$  arc s. The specimen crystal is aligned in the (+, -, -, +) configuration. Due to dispersive configuration, though the lattice constant of the monochromator crystal(s) and the specimen are different, the unwanted dispersion broadening in the diffraction curve of the specimen crystal is insignificant. The specimen can be rotated about a vertical axis, which is perpendicular to the plane of diffraction, with minimum angular interval of 0.5 arc s. The diffracted intensity is measured by using a scintillation counter. The DCs were recorded by changing the glancing angle (angle between the incident X-ray beam and the surface of the specimen) around the Bragg diffraction peak position  $\theta_B$  (taken zero as reference point) starting from a suitable arbitrary glancing angle ( $\theta$ ). The detector was kept at the same angular position  $2\theta_B$  with wide opening for its slit, the so-called  $\omega$  scan. For all the specimens of the present study, the X-ray power, size of the beam, configuration of the diffractometer was kept

constant. Before recording the diffraction curve, to remove the non-crystallized solute atoms remained on the surface of the crystal and also to ensure the surface planarity, the specimens were first lapped and chemically etched in a non preferential etchant of water and acetone mixture in 1:2 volume ratio.

## Results and discussion

#### FT-IR spectral analysis

Comparison of the characteristic vibrational frequencies of pure KHP and Os(VIII)-doped crystals reveals a very slight shift in some of the vibrational frequencies. It could be due to the lattice strain as a result of doping.

#### XRD analysis

X-ray diffraction was performed at room temperature using a wavelength of 1.540 Å with a step size of 0.008°. The powder XRD patterns of Os(VIII) doped KHP samples are compared with that of undoped one (Fig. 2). The spectra show some interesting features. No new peaks or phases were observed by doping with transition metal osmium. However, a drastic reduction in intensity is observed as a result of doping. The slight structural changes indicate the lattice strain due to the doping. The granularity is decreased from ~48 nm for pure KHP to ~30 nm for doped specimen.

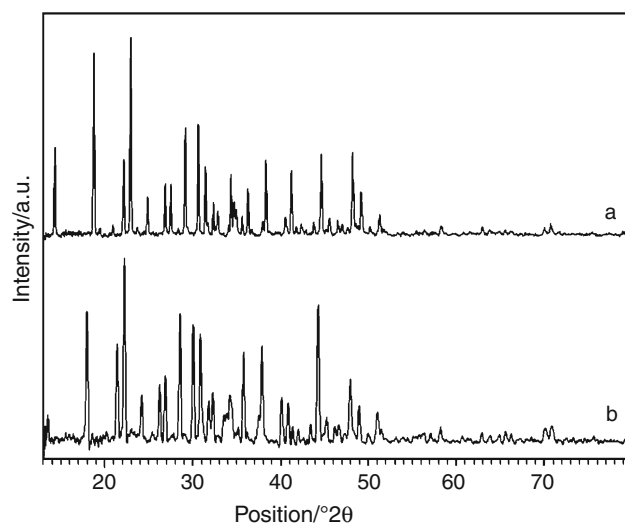


**Fig. 2** Powder X-ray diffraction curves of KHP crystals (a) pure and (b) 1 mol% OsO<sub>4</sub> doped

## SEM

The effect of the influence of dopants on the surface morphology of KHP crystal faces reveals structure defect centers as seen in the SEM images (Fig. 3). The plate morphology was observed for pure KHP. Doping results in defect centers and crystal voids with reduction of grain size. The present and the earlier studies [47] on doped KHP crystals indicate that the dopants lead to mosaicity in them.

## Thermal (TG–DTA–DSC) analysis

The DSC analysis clearly shows that there is no physically adsorbed water in the molecular structure of crystals. The studies reveal the purity of the material. DSC (Fig. 4b) shows that the melting point of doped crystal is 305 °C. The compound is stable and there is no phase transition till it is melting. No decomposition up to the melting point ensures the suitability of the material for application in lasers where the crystals are required to withstand high temperatures. It is interesting to observe that the small quantity addition of doped material makes the crystal melts at a higher temperature (305 °C) than the pure specimen (296 °C, Fig. 4a) implying enhanced mechanical stability. It roughly suggests that there is some interaction between the host crystal and the dopant.

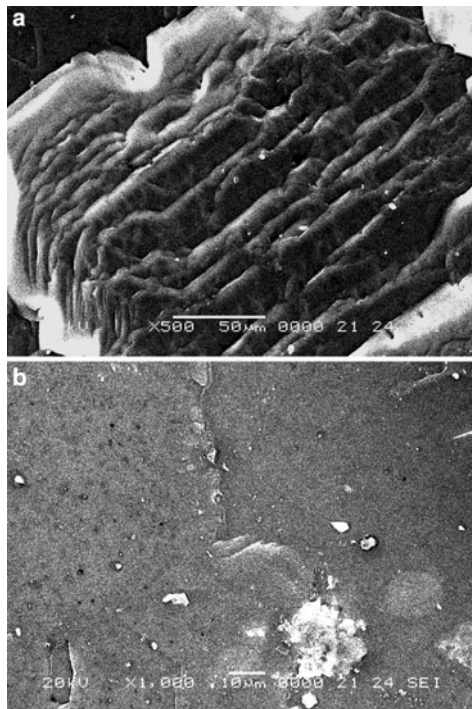


**Fig. 3** SEM images of KHP crystals **a** pure and **b** 1 mol%  $\text{OsO}_4$  doped

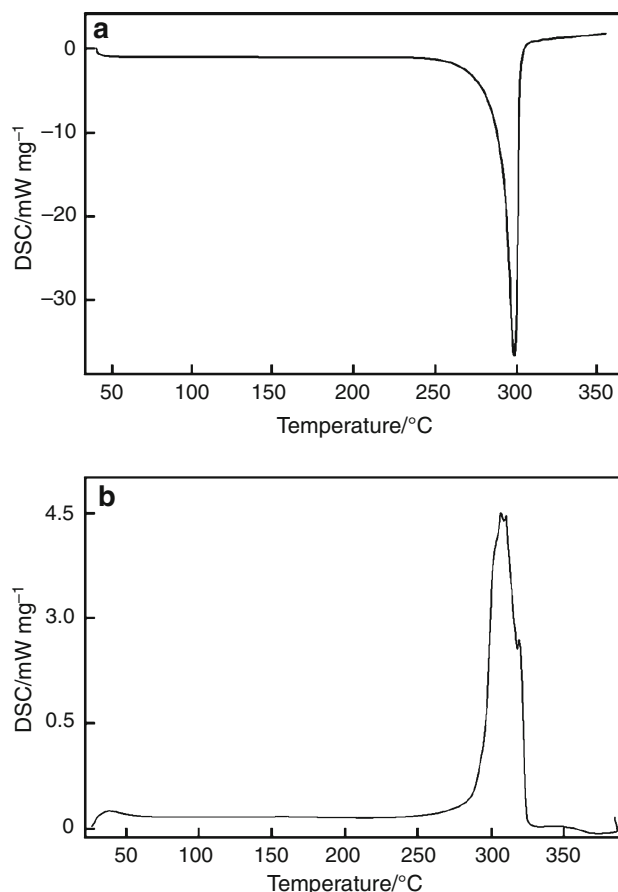


**Fig. 4** DSC curves of **a** pure KHP and **b** 1 mol%  $\text{OsO}_4$ -doped KHP

The TG curve provides with a quantitative measurement of mass change associated with the transition. It indicates that on melting the material decomposes and loses mass. The curve shows a gradual mass loss. The sharpness of the endothermic peaks shows good degree of crystallinity of the grown ingot. The TG curve (Fig. 5b) shows three mass loss processes at inflection temperatures 293, 520, and 948 °C. These processes were accompanied by total mass losses of 43, 13, and 32 mass%. The DTA curve shows four endothermic peaks at 178, 300, 430, and 957 °C.

## UV–Vis and PL spectral studies

The UV spectrum reveals that the cut off wavelength is  $\sim 300$  nm. Absorption is minimum in the 300–1,100 nm region. It appears that the doping does not destroy the optical transmission. No significant  $\lambda_{\text{max}}$  shift is observed but the absorbance is reduced drastically by doping. As seen in Table 1 and Fig. 6, PL spectrum clearly reveals the complex formation in the case of Os(VIII)-doping since  $\lambda_{\text{flu}}$  undergoes blue shift, i.e., from 435 to 419 nm. The Os(VIII) enhances the fluorescence significantly and it acts as an antenna ligand. Intramolecular energy transfer is well

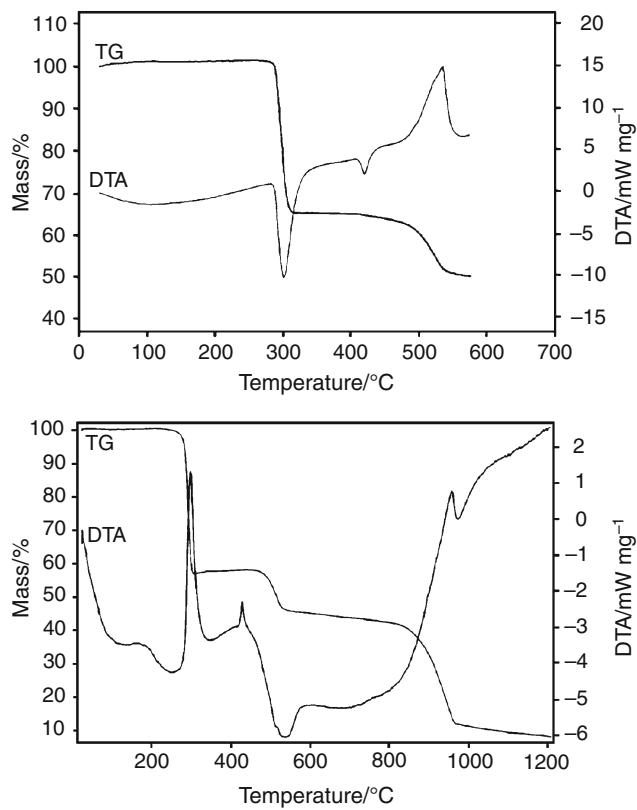


**Fig. 5** TG-DTA curves of **a** pure KHP and **b** 1 mol%  $\text{OsO}_4$ -doped KHP

facilitated in the presence of Os(VIII) and this could be the main reason for the enhanced fluorescence intensity.

#### SHG efficiency

In the SHG test performed on the powder samples, the input radiation was 2.5 mJ/pulse. The output SHG intensities (Table 2) for pure and doped specimens give relative NLO efficiencies of the measured specimens. Depressed SHG output in the case of doping with heavy transition metal (Os) is quite likely due to the deterioration of crystalline perfection that might be lead to the disturbance of charge transfer.

#### HRXRD analysis

The effect of crystalline perfection due to incorporation of dopants in the crystalline matrix of the grown crystals was

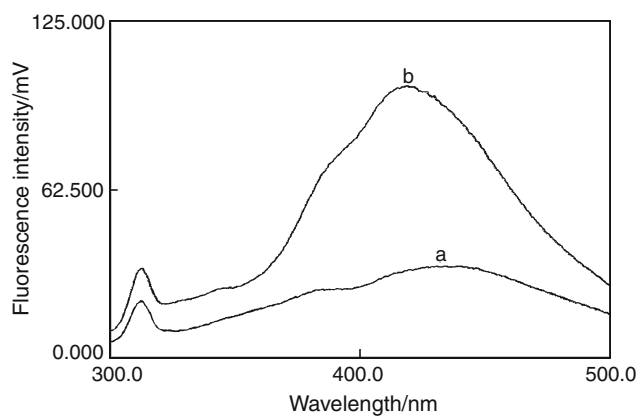


**Fig. 6** PL spectra of KHP crystals **(a)** pure and **(b)** 1 mol%  $\text{OsO}_4$  doped

**Table 2** SHG output

System	$I_{2\omega}/\text{mV}$
Pure KHP	27–29
1 mol% $\text{OsO}_4$ -doped KHP	21–23

evaluated by HRXRD studies by employing the multi-crystal X-ray diffractometer developed at NPL. Figure 7a shows the high-resolution X-ray (DC) for the undoped KHP crystal recorded for (010) diffracting planes using  $\text{MoK}\alpha_1$  radiation in symmetrical Bragg geometry. The curve is quite sharp having full width at half maximum (FWHM) of 13 arc s with a good symmetry with respect to the exact diffraction peak position (taken as zero) as expected for a nearly perfect crystal from the plane wave dynamical theory of X-ray diffraction [48].

Figure 7b shows the DC recorded for doped KHP crystals using (010) diffracting planes in symmetrical Bragg geometry under the same experimental conditions as that of Fig. 7a. These curves were drawn after removing a few micron thick surface layers from specimen. The Os(VIII) doped crystals of KHP do not contain any additional peaks and have FWHM value of 23 arc s. The relatively sharp and single peaks of these curves show that these crystals do not contain any structural grain boundaries and the crystalline perfection is reasonably good. However, due to large stress, the crystal develops structural grain boundaries and the dopants segregate along the boundaries by the process of guttering as observed in oxalic acid-doped ADP crystals [14]. Though the specimen belongs to Os(VIII) doping at 1 mol% doping level does not contain the boundaries as seen in the Fig. 7b, on careful observation, one can see that the DC has an asymmetry with respect to the peak Os(VIII) position having more scattered intensity on the higher glancing angle side than that on the lower glancing angle side for a particular deviation angle ( $\Delta\theta$ ) from the zero

**Table 1** Fluorescence output

System	$\lambda_{\text{flu}}$	Intensity
KHP pure	435.0	41.765
KHP/ $\text{OsO}_4$ doped	419.0	100.827

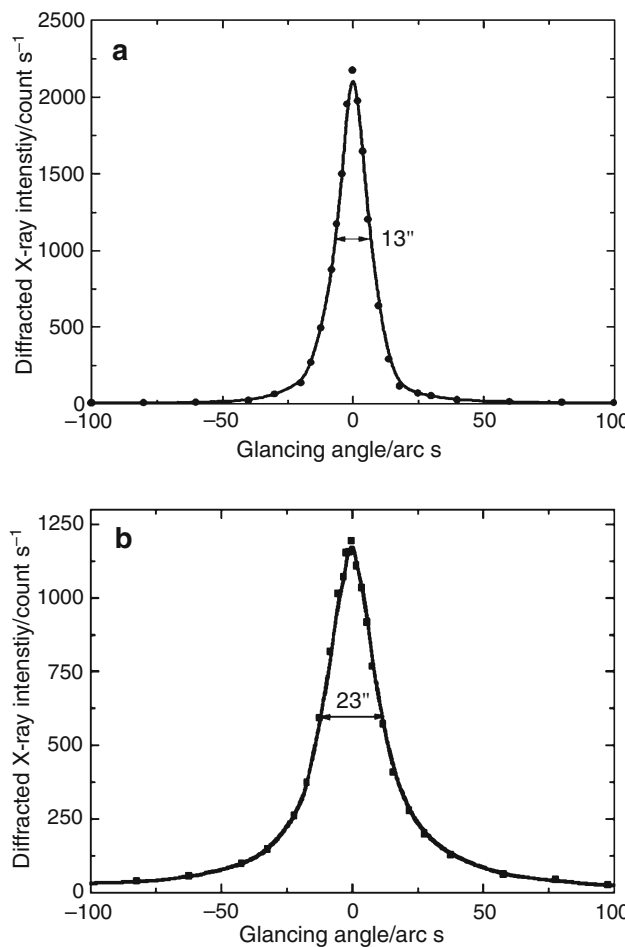


**Fig. 7** **a** High-resolution XRD curve recorded in symmetrical Bragg geometry for an undoped KHP crystal specimen using (010) planes and **b** XRD curve recorded for typical KHP crystals using (010) diffracting planes with 1 mol% doping of OsO<sub>4</sub>

position indicating that Os(VIII) takes the interstitial positions. The charge density in Os(VIII) is high (because of small size and high valence) and it is interesting to observe that it prefers interstitial sites rather than substitutional positions. Our previous investigations on KHP crystals [13] also revealed that the transition metal predominantly occupies the interstitial positions.

## Conclusions

We have used XRD, SEM, EDS, HRXRD, TG-DTA-DSC, and FT-IR, UV-Vis and PL spectra and Kurtz powder techniques to study the influence of doping with high valence transition metal Os on KHP crystals. A close observation of XRD profiles of doped and undoped samples reveals some minor structural variations. The studies indicate that the crystal undergoes considerable lattice stress as a result of doping. It is clear from the HRXRD

investigations that this high valence heavy transition metal mainly occupies the interstitial sites. Complex formation is clearly evidenced by PL spectra in the Os(VIII) doping and it also enhances the emission intensity. The Os(VIII) doping results in depressed SHG efficiency quite likely owing to the disturbance of charge transfer.

**Acknowledgements** One of the authors GB acknowledges Dr. Vikram Kumar, Director, NPL and Dr. B. R. Chakraborti for their constant encouragement to carry out the present investigations. The authors are grateful to the authorities of Annamalai University for providing the experimental facilities used in the present investigation.

## References

1. Jones JL, Paschen KW, Nicholson JB. Performance of curved crystals in the range 3 to 12 Å. *J Appl Opt.* 1963;2:955–61.
2. Yoda O, Miyashita A, Murakami K, Aoki S, Yamaguchi N. Time-resolved X-ray absorption spectroscopy apparatus using laser plasma as an X-ray source. *Proc SPIE Int Soc Opt Eng.* 1991;1503:463–6.
3. Miniewicz A, Bartkiewicz S. On the electro-optic properties of single crystals of sodium, potassium and rubidium acid phthalates. *Adv Mater Opt Electron.* 1993;2:157–63.
4. Kejalakshmy N, Srinivasan K. Growth, optical and electro-optical characterisations of potassium hydrogen phthalate crystals doped with Fe<sup>3+</sup> and Cr<sup>3+</sup> ions. *Opt Mater.* 2004;27:389–94.
5. Shankar MV, Varma KBR. Piezoelectric resonance in KAP single crystals. *Ferroelectr Lett Sect.* 1996;21:55–9.
6. Okaya Y. The crystal structure of potassium acid phthalate, KC<sub>6</sub>H<sub>4</sub>COOH·COO. *Acta Crystallogr.* 1965;19:879–82.
7. Nisoli M, Pruner V, Magni V, De Silvestri S, Dellepiane G, Cuniberti DC, et al. Ultrafast exciton dynamics in highly oriented polydiacetylene films. *Appl Phys Lett.* 1994;65:590–3.
8. Timpanaro S, Sassella A, Borghesi A, Porzio W, Fountaine P, Goldmann M. Crystal structure of epitaxial quaterthiophene thin films grown on potassium acid phthalate. *Adv Mater.* 2001;13: 127–30.
9. Van Enckevort WJP, Jetten LAMJ. Surface morphology of the 010 faces of potassium hydrogen phthalate crystals. *J Cryst Growth.* 1982;60:275–85.
10. Ester GR, Price R, Halfpenny PJ. An atomic force microscopic investigation of surface degradation of potassium hydrogen phthalate (KAP) crystals caused by removal from solution. *J Cryst Growth.* 1997;182:95–102.
11. Murugakoothan P, Mohankumar R, Ushashree PM, Jayavel R, Dhanasekaran R, Ramasamy P. Habit modification of potassium acid phthalate (KAP) single crystals by impurities. *J Cryst Growth.* 1999;207:325–9.
12. Santos VP, Tremiliosi-Filho G. Effect of osmium coverage on platinum single crystals in the ethanol electrooxidation. *J Electroanal Chem.* 2003;554:395–405.
13. Bhagavannarayana G, Parthiban S, Chandrasekaran C, Meenakshisundaram S. Effect of alkaline earth and transition metals doping on the properties and crystalline perfection of potassium hydrogen phthalate (KHP) crystals. *CrystEngComm.* 2009;11: 1635–41.
14. Bhagavannarayana G, Parthiban S, Meenakshisundaram S. An interesting correlation between crystalline perfection and second harmonic generation efficiency on KCl- and oxalic acid-doped ADP crystals. *Cryst Growth Des.* 2008;8:446–51.
15. Bhagavannarayana G, Kushwaha SK, Parthiban S, Meenakshisundaram S. The influence of Mn-doping on the nonlinear optical

- properties and crystalline perfection of tris(thiourea)zinc(II) sulphate crystals: concentration effects. *J Cryst Growth.* 2009;311: 960–5.
16. Meenakshisundram S, Parthiban S, Bhagavannarayana G, Madhurambal G, Mojumdar SC. Influence of organic solvent on trithioureazinc(II)sulphate crystals. *J Therm Anal Calorim.* 2009;96:125–9.
  17. Swiderski G, Kalinowska M, Wojtulewski S, Lewandowski W. Experimental (FT-IR, FT-Raman,  $^1\text{H}$  NMR) and theoretical study of magnesium, calcium, strontium, and barium picolimates. *Spectrochim Acta A.* 2006;64:24–33.
  18. Flakus HT, Jablonska M. Study of hydrogen bond polarized IR spectra of cinnamic acid crystals. *J Mol Struct.* 2004;707:97–108.
  19. Hanai K, Kuwae A, Takai T, Senda H, Kunimoto K. A comparative vibrational and NMR study of cis-cinnamic acid polymorphs and trans-cinnamic acid. *Spectrochim Acta A.* 2001;57: 513–9.
  20. Hsich T, Su C, Su C, Chen C, Liou CH, Li-Hwa L. Using experimental studies and theoretical calculations to analyze the molecular mechanism of coumarin, p-hydroxybenzoic acid, and cinnamic acid. *J Mol Struct.* 2005;741:193–9.
  21. Vasudevan G, Anbusrinivasan P, Madhurambal G, Mojumdar SC. Thermal analysis, effect of dopants, spectral characterisation and growth aspects of KAP crystals. *J Therm Anal Calorim.* 2009;96:99–102.
  22. Julg A, Francois P. Recherches sur la géométrie de quelques hydrocarbures non-alternants: son influence sur les énergies de transition, une nouvelle définition de l'aromaticité. *Theor Chim Acta.* 1967;8:249–59.
  23. Kalinowska M, Siemieniuk E, Kostro A, Lewandowski W. The application of Aj, BAC, I<sub>6</sub>, HOMA indexes for quantitative determination of aromaticity of metal complexes with benzoic, salicylic, nicotinic acids and benzene derivatives. *J Mol Struct.* 2006;761:129–41.
  24. Anbusrinivasan P, Madhurambal G, Mojumdar SC. p-N, N-dimethylaminobenzaldehyde (DAB) grown by solution technique using CCl<sub>4</sub> as growth medium. *J Therm Anal Calorim.* 2009; 96: 111–5.
  25. Varsanyi G. Assignments for vibrational spectra of 700 benzene derivatives. Budapest: Akademiai Kiado; 1973.
  26. Reva ID, Stepanian SG. An infrared study on matrix-isolated benzoic acid. *J Mol Struct.* 1995;349:337–40.
  27. Spanian SG, Reva ID, Radchenko ED, Sheina GG. Infrared spectra of benzoic acid monomers and dimers in argon matrix. *Vib Spectrosc.* 1996;11:123–33.
  28. Wienda DA, Feng TL, Barron AR. Structure of  $\alpha$ -trans-cinnamic acid. *Acta Crystallogr C.* 1989;45:338–9.
  29. Bryan RF, Fryberg DP. Crystal structures of  $\alpha$ -trans- and p-methoxy-cinnamic acids and their relation to thermal mesomorphism. *J Chem Soc Perkin Trans.* 1975;2:1835–40.
  30. Madhurambal G, Mojumdar SC, Hariharan S, Ramasamy P, TG, DTC, FT-IR and Raman spectral analysis of Zn<sub>a</sub>/Mg<sub>b</sub> ammonium sulfate mixed crystals. *J Therm Anal Calorim.* 2004;78:125–33.
  31. Lewandowski W, Dasiewicz B, Koczon P, Skierski J, Dobrosz-Teperek K, Swislocka R, et al. Vibrational study of alkaline metal nicotinates, benzoates and salicylates. *J Mol Struct.* 2002;604: 189–93.
  32. Varshney G, Agrawal A, Mojumdar SC. Pyridine based cerium(IV) phosphate hybrid fibrous ion exchanger: Synthesis, characterization and thermal behaviour. *J Therm Anal Calorim.* 2007;90:731–4.
  33. Dichi P, Kellerhals M, Lounila J, Wasser R, Hiltunen Y, Jokisari J, et al. NMR structure of partially oriented tellurophene: correction of molecular deformations and determination of bond interaction parameters. *Magn Res Chem.* 2005;25:244–7.
  34. Mojumdar SC. Thermoanalytical and IR-spectral investigation of Mg(II) complexes with heterocyclic ligands. *J Therm Anal Calorim.* 2001;64:629–36.
  35. Chenthamarai S, Jayaraman D, Meera K, Santhanaraghavan P, Subramanian C, Bocelli G, Ramasamy P. Growth and single crystal XRD characterization of undoped and doped 4-hydroxyacetophenone. *Cryst Eng.* 2001;4:37–48.
  36. Hameed SH, Ravi G, Dhanasekaran R, Ramasamy P. Studies on organic indole-3-aldehyde single crystals. *J Cryst Growth.* 2000; 212:227–32.
  37. Patel RN, Pandeya KB. Specific displacement of glutathione from the Pt(II)-glutathione adduct by Cu(II) in neutral phosphate buffer. *J Inorg Biochem.* 1998;71:109–13.
  38. Mojumdar SC, Madhurambal G, Saleh MT. A study on synthesis and thermal, spectral and biological properties of carboxylato-Mg(II) and carboxylate-Cu(II) complexes with bioactive ligands. *J Therm Anal Calorim.* 2005;81:205–10.
  39. Rathore HS, Varshney G, Mojumdar SC, Saleh MT. Synthesis, characterization and fungicidal activity of zinc diethyldithiocarbamate and phosphate. *J Therm Anal Calorim.* 2007;90:681–6.
  40. Mojumdar SC, Sain M, Prasad RC, Sun L, Venart JES. Selected thermoanalytical methods and their applications from medicine to construction. *J Therm Anal Calorim.* 2007;90:653–62.
  41. Mojumdar SC, Lebruskova K, Valigura D. Thermal stability and spectral properties of pyrazine-2,3-dicarboxylatocuppper(II) complexes with ronicol. *Chem Pap.* 2003;57:245–9.
  42. Mojumdar SC, Capek I, Capek P, Fialova L, Berek D. Preparation of composite nanoparticles on the base of starch. *Res J Chem Environ.* 2007;11:5–12.
  43. Meenakshisundaram S, Parthiban S, Sarathi N, Kalavathy R, Bhagavannarayana G. Effect of organic dopants on ZTS single crystals. *J Cryst Growth.* 2006;293:376–81.
  44. Kuznetsov VA, Okhrimenko TM, Rak M. Growth promoting effect of organic impurities on growth kinetics of KAP and KDP crystals. *J Cryst Growth.* 1998;193:164–73.
  45. Kurtz SK, Perry TT. A powder technique for the evaluation of nonlinear optical materials. *J Appl Phys.* 1968;39:3798–813.
  46. Lal K, Bhagavannarayana G. A high-resolution diffuse X-ray scattering study of defects in dislocation-free silicon crystals growth by the float-zone method and comparison with Czochralski-grown crystals. *J Appl Cryst.* 1989;22:209–15.
  47. Bhagavannarayana G, Parthiban S, Meenakshisundaram SP. Enhancement of crystalline perfection by organic dopants in ZTS, ADP and KHP crystals as investigated by high-resolution XRD and SEM. *J Appl Crystallogr.* 2006;39:784–90.
  48. Batterman BW, Cole H. Dynamical diffraction of X rays by perfect crystals. *Rev Mod Phys.* 1964;36:681–717.